Biochemical and Biophysical Research Communications 461 (2015) 372–377

Contents lists available at ScienceDirect

Biochemical and Biophysical Research Communications

journal homepage: www.elsevier.com/locate/ybbrc

Micropillar displacements by cell traction forces are mechanically correlated with nuclear dynamics

Qingsen Li [a, 1], Ekta Makhija [a, 1], F.M. Hameed [a], G.V. Shivashankar [a, b, *]

[a] Mechanobiology Institute, National University of Singapore, Singapore
[b] Department of Biological Sciences, National University of Singapore, Singapore

ARTICLE INFO

Article history:
Received 27 March 2015
Available online 22 April 2015

Keywords:
Micropillars
Mechanotransducion
Correlation
Nuclear dynamics
Focal adhesion

ABSTRACT

Cells sense physical cues at the level of focal adhesions and transduce them to the nucleus by biochemical and mechanical pathways. While the molecular intermediates in the mechanical links have been well studied, their dynamic coupling is poorly understood. In this study, fibroblast cells were adhered to micropillar arrays to probe correlations in the physical coupling between focal adhesions and nucleus. For this, we used novel imaging setup to simultaneously visualize micropillar deflections and EGFP labeled chromatin structure at high spatial and temporal resolution. We observed that micropillar deflections, depending on their relative positions, were positively or negatively correlated to nuclear and heterochromatin movements. Our results measuring the time scales between micropillar deflections and nucleus centroid displacement are suggestive of a strong elastic coupling that mediates differential force transmission to the nucleus.

© 2015 Elsevier Inc. All rights reserved.

1. Introduction

Eukaryotic cells probe the stiffness of their local microenvironment to modulate gene expression and determine lineage specification [1]. Mechanical cues from the environment such as substrate rigidity [2], geometry [3,4] and force [5] impinge on cellular gene expression via biochemical and mechanical pathways. Towards this, forces are applied on the substrate by focal adhesions using acto-myosin contraction [6] and these substrate signals are then transmitted to the nucleus. While the biochemical pathways have been studied in detail over the past few years, physical links are only recently being explored [7–12].

The physical link from focal adhesions to the nucleus is mediated via cytoskeleton proteins, linkers of nucleoskeleton complex proteins and lamins [13–17]. To understand the viscoelastic nature of this mechanical coupling, various groups including ours [7,10–12] have measured the nuclear displacements and deformations upon perturbations of cytoskeletal and nuclear links or application of extracellular shear and compressive forces. However, the intrinsic time scales of focal adhesion to nucleus coupling, in unperturbed cells are yet unknown.

In this study, we probed the intrinsic coupling between micropillar array deflections induced by traction forces at focal adhesions and the resultant displacements of the nucleus and heterochromatin foci. Microfabricated pillar arrays, when used as substrate for cells, act as cantilever beams and their deflections can be used to calculate magnitude and direction of cell traction forces [18]. The tips of these micropillars have been shown to form focal adhesions [19]. Such micropillar deflections provide a measure for mapping force transduction from focal adhesions to the nucleus.

2. Materials and methods

2.1. Preparation of PDMS micropillars

PDMS micropillars were prepared from PDMS Elastomer Kit (SYLGARD 184, DOW Corning). The curing agent and precursor were mixed homogenously in the ratio 1:10 and then poured onto the micropillar array mould in a silicon wafer followed by curing at 80 °C for 2 h. The micropillars so formed were 2 μm in diameter, 5 μm in height with pillar centre to centre distance of 3 μm as confirmed by electron microscopy imaging.

* Corresponding author. Mechanobiology Institute, National University of Singapore, Singapore.
E-mail address: shiva.gvs@gmail.com (G.V. Shivashankar).
[1] These authors contributed equally to this work.

http://dx.doi.org/10.1016/j.bbrc.2015.04.041
0006-291X/© 2015 Elsevier Inc. All rights reserved.

2.2. Stamping of micropillars with fibronectin

30 μl of 100 μg/ml fibronectin solution was deposited on a flat PDMS block substrate for 10 min. The solution was then removed and the block dried for 5 min. The stamp was then inverted over the UV treated micropillars for 5 min. The stamp was then removed and the PDMS micropillars washed with PBS and further treated with 1 ml of 2 mg/ml Pluronic F-127 (Sigma) for 2 h to passivate non-fibronectin coated regions

2.3. Cell culture, transfection and seeding

NIH3T3 cells were cultured in low glucose DMEM supplemented with 10% FBS and 1% Penicillin-Streptomycin. Transfections were carried out with fusion plasmid for core histone H2B tagged with EGFP and lifeact mRFP using Jetprime transfection reagent (Polyplus). All cell culture reagents were from GIBCO Invitrogen. Cells were seeded on fibronectin coated PDMS micropillar arrays and allowed to spread for 12 h before being inverted over coverslip dishes for imaging.

2.4. Live imaging

All images were captured using inverted confocal microscope (Perkin Elmer Spinning Disk, 60X, 1.2 NA objective) at 1 frame every 3–7 s for at least 3 min. The PDMS micropillars were placed upside down on glass bottom petridish (Ibidi) with a 60 μm thick PDMS membrane placed at the edges of PDMS pillar block as spacer.

2.5. Pillar deflection and nuclear movement measurements

The deflections of the pillar tips and the nucleus and the heterochromatin foci were calculated using custom code written in MATLAB. The tips of the pillars show up as bright spots in the bright field images. To calculate the position of the pillar tips, bright field pillar images were thresholded and centroid was calculated for each time point. The images were corrected for XY drift using the mean displacement of pillars not in contact with the cell. A square lattice was generated by calculating the distance between adjacent pillars from the control region. The lattice was then best fit to the cell region so as to minimize the deflection of pillars outside the cell. The centroid of the nuclei was obtained by thresholding for H2B-EGFP and calculating the centroid in ImageJ. The centroids of the heterochromatin were obtained by utilizing the same method after cropping out everything but the heterochromatin foci.

2.6. Correlation analysis

The time series were analyzed for autocorrelation and cross correlation using custom written code in MATLAB. The autocorrelations of the displacement (magnitude) of the pillar, the nucleus, and heterochromatin foci were calculated and plotted to arrive at their typical timescales. Further, the cross correlations between displacements (component along direction of nucleus movement) of individual micropillars at different regions under the cell were plotted with respect to the displacements (component along direction of nucleus movement) of nucleus and heterochromatin foci.

3. Results

3.1. Micropillar deflections map spatial distribution of cell matrix interactions

NIH3T3 fibroblast cells stably expressing H2B-EGFP were allowed to spread for 12 h on force sensitive micropillar arrays.

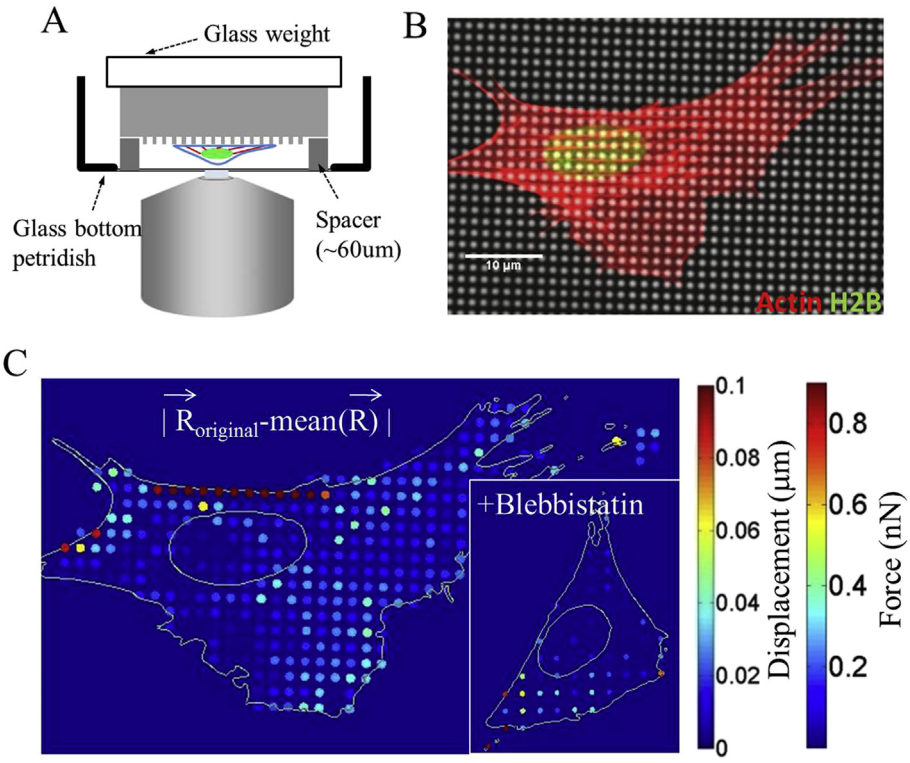

Fig. 1. Experimental setup. A) Inverted imaging configuration B) Image of pillars, H2B-EGFP nucleus and lifeact-RFP actin C) Color coded pillar deflections and corresponding force magnitude. Inset shows similar results for cell treated with blebbistatin.

Simultaneous time-lapse imaging under bright field for pillars and EGFP fluorescence for chromatin was carried out. The imaging setup consisted of the cells plated on micropillars placed upside down on glass bottom dishes, with 60 μm thick PDMS spacers at the edges (Fig. 1A). This inverted setup has dual advantages. First, it provides direct access to the high NA objective with short working distance. Second, it prevents the imaging artifacts caused by interference of fluorescence beam passing through the micropillars. A representative image of micropillars, H2B-EGFP labeled cell nucleus and lifeact-RFP labeled F-actin is shown in Fig. 1B (Supp movie 1 and 2). The centroids of all micropillars under the cell (cell region) and those away from it (control region) were tracked over time using custom written code in MATLAB. The original position of pillars under the cell was calculated by fitting a square lattice (distance between pillars calculated using control region) to minimize the deflections of pillars outside the cell [18]. The distance between the original position and the mean observed position of each pillar was measured as the pillar deflection and was used to calculate the magnitude of force on each pillar (Fig. 1C). The maximum pillar deflections were of the order of few hundred nm, corresponding to forces of order of few nN (consistent with previous reports [20]).

Supplementary data related to this article can be found online at http://dx.doi.org/10.1016/j.bbrc.2015.04.041.

Typical pillar centroid trajectories and fluctuations in the cell and control regions are shown in Fig. 2A and B. A histogram of pillar

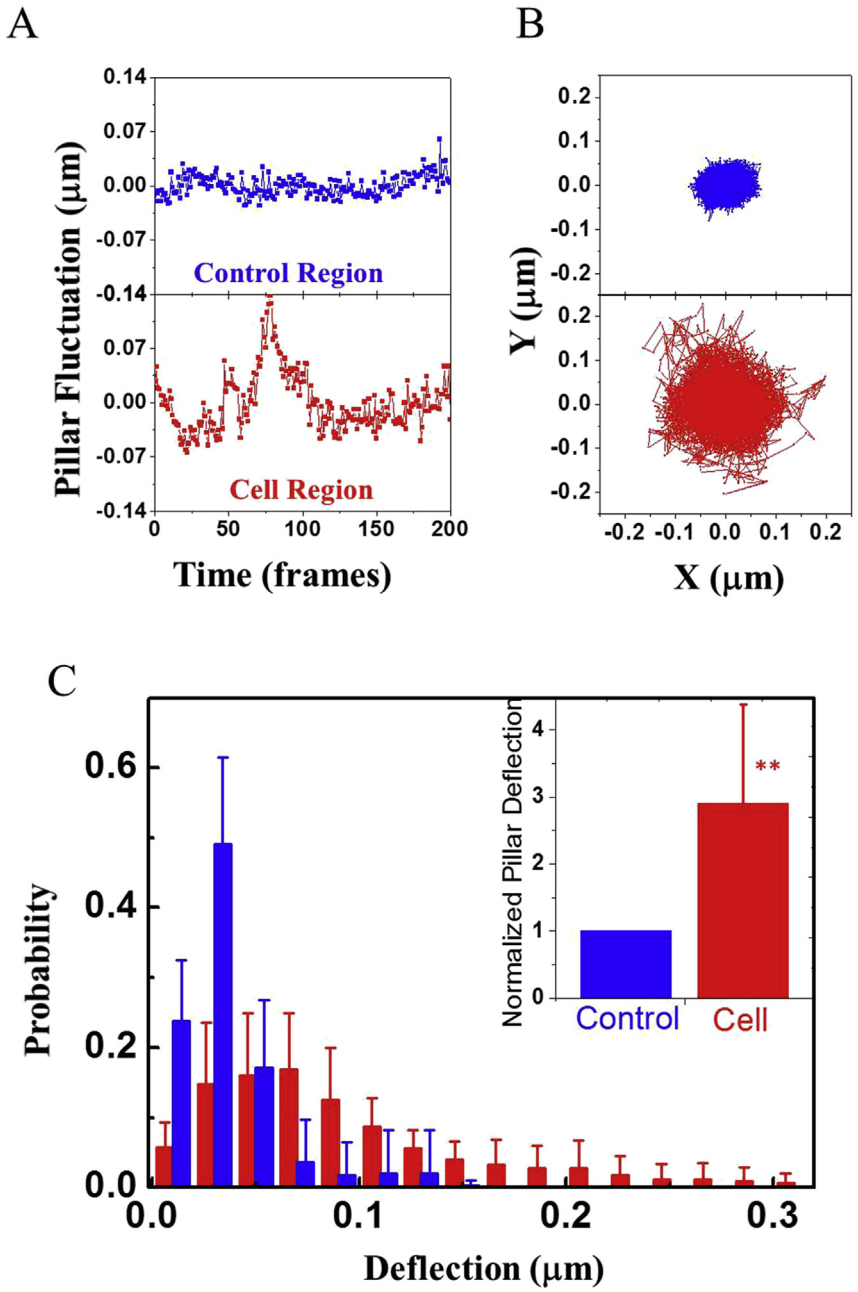

Fig. 2. Pillar tracking and validation. A) Typical pillar fluctuation B) XY traces in control and cell regions. Time between frames is 3 s. C) Histogram of pillar deflections in control and cell regions. Inset shows mean pillar deflection normalized with respect to control region. Error bars represent standard deviation.

displacements under the cell (Fig. 2C) shows significantly larger displacements of pillars (maximum up to ~300 nm) due to cell traction forces than those in the control region. Consistent with this, myosin inhibited (using blebbistatin) cells exhibit lower pillar deflections, closer to that of control regions (Supp Fig. 1 and Fig. 1C inset).

3.2. Dynamic correlations between micropillar and nuclear displacements

In order to probe the dynamic correlation between micropillars and nuclear displacements, we carried out autocorrelation and cross correlation analysis. The autocorrelation analysis provides a direct measure of the underlying active cellular processes driving pillar and nuclear displacements. Autocorrelation function was plotted for the magnitude of displacement of individual pillars in the control and cell regions (Fig. 3A). The movement of pillars due to cell traction forces exhibited a decorrelation time scale ~40 s. As expected, the autocorrelation curves for the pillars in control region were observed to drop sharply. We then evaluated the autocorrelation function for the nucleus and heterochromatin foci displacement magnitudes and noticed similar time scales (Fig. 3B). In addition, the mean square displacement of the nucleus is shown in Supp Fig. 2. These results suggest an elastic nature of the architectural coupling between the focal adhesions and the nucleus.

We then carried out cross-correlation analysis between pillar displacements and the movement of the nucleus and heterochromatin foci (component along direction of nucleus movement) to investigate the spatiotemporal nature of their viscoelastic coupling. We observed that the micropillar deflections under different regions of the cell were distinct (Supp Fig. 3, supp movie 3). Pillars at the leading edge showed a negative correlation with the movement of the nucleus while those at the rear edge showed a positive correlation (Fig. 4A). These results showed a minimal time lag in the cross correlation between pillar and nuclear movements. As expected, the cross correlation between the pillars in the leading edge of the cell vs those at the lagging edge show complete anticorrelation (Supp Fig. 4). Further, calculation of the angle between pillar deflection and nucleus movement (Fig. 4B and C) showed that pillars in the front edge deflect back towards the nucleus (angle ~ 180°) while those at the rear edge deflect forward towards the nucleus (angle ~ 0°). Upon myosin inhibition with blebbistatin treatment, this distinct correlation is partially lost (Fig. 4C inset).

Supplementary data related to this article can be found online at http://dx.doi.org/10.1016/j.bbrc.2015.04.041.

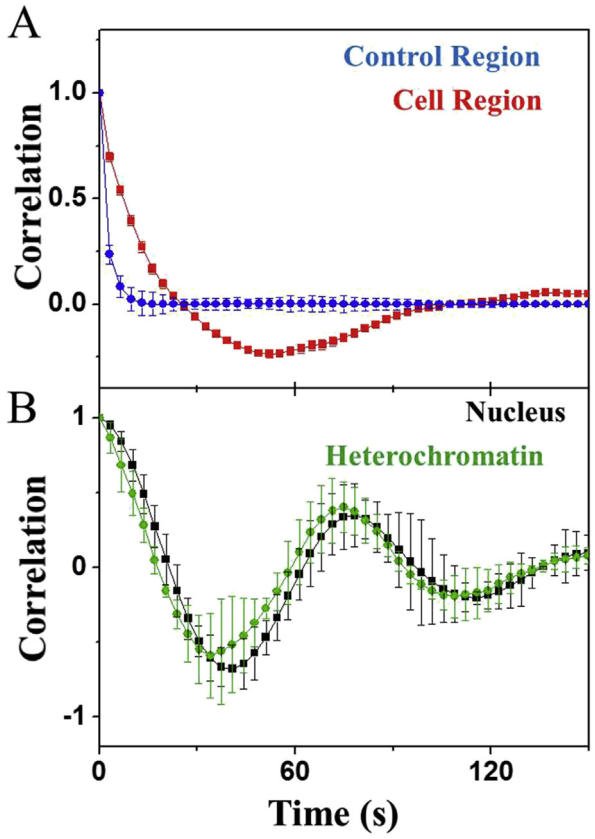

Fig. 3. Autocorrelation analysis. A) Typical autocorrelation function of pillars in control and cell regions obtained by using micropillar deflection time series B) Autocorrelation function of nucleus centroid and heterochromatin foci displacement time series.

4. Discussion

In summary, this work investigates the intrinsic nature of coupling between focal adhesions and nucleus cultured on micropillars. We carried out simultaneous imaging of pillar deflections and nucleus and heterochromatin foci dynamics and then performed autocorrelation and cross-correlation analysis for these displacements. The autocorrelation time scales were similar (~40 s) for both pillar and nuclear displacements. This time scale is close to the time scale of fibroblast cell contraction, i.e. 1 min [21], suggesting that the coupling between pillar and nucleus is mediated by cytoskeletal contraction. Secondly, the maximum cross-correlation between pillar and nuclear displacements was observed at lag time less than 1 s. The response time for a purely elastic system, calculated by dividing the distance from cell edge to nucleus (~10 μm) with the speed of mechanical stress wave propagation along tensed cytoskeletal filaments (~30 m/s, [22]) is less than a microsecond. For a viscoelastic system, the response time as calculated by the ratio of cytoplasmic viscosity (~15 Poise, [23]) to cytoplasmic elastic modulus (~150 dyn/cm^2, [23]) is one-tenth of a second. However, for a purely viscous system, the response time calculated by dividing the distance from cell edge to nucleus (~10 μm) with the speed of wave propagation (~speed of pillar displacement, i.e. 0.1 μm/25s = 4 nm/s, Fig. 2A, neglecting the cytoplasmic viscous drag) is much longer and of the order of ~40 min. In the presence of a retrograde flow (10 nm/s [24]), this response time decreases to ~10 min. Comparing these numbers with the lag time of pillar-nucleus cross-correlation, we conclude that the mechanical links between focal adhesions and nucleus in living cells must have a strong elastic component. A recent report [25] also revealed that the cytoplasm behaves as an elastic gel by analyzing motion of injected particles inside the cell. Further, the spatial maps of pillar displacements and their correlations showed distribution of active forces exerted by cells on the substrate. The spatial heterogeneity in pillar displacements with respect to nuclear movements possibly suggest a highly coordinated contractile process to test local microenvironment during cell migration. As a result, myosin inhibition using blebbistatin inhibited such spatial correlation. Our observed force transduction time scales suggest that chromatin structure could respond rapidly to local microenvironment signals thus facilitating better integration of biochemical pathways to the nucleus. Collectively, our studies reveal that cells are constantly testing the local microenvironment using actomyosin contractility and instantaneously transmit such mechanical signals to the nucleus to possibly maintain cellular homeostasis.

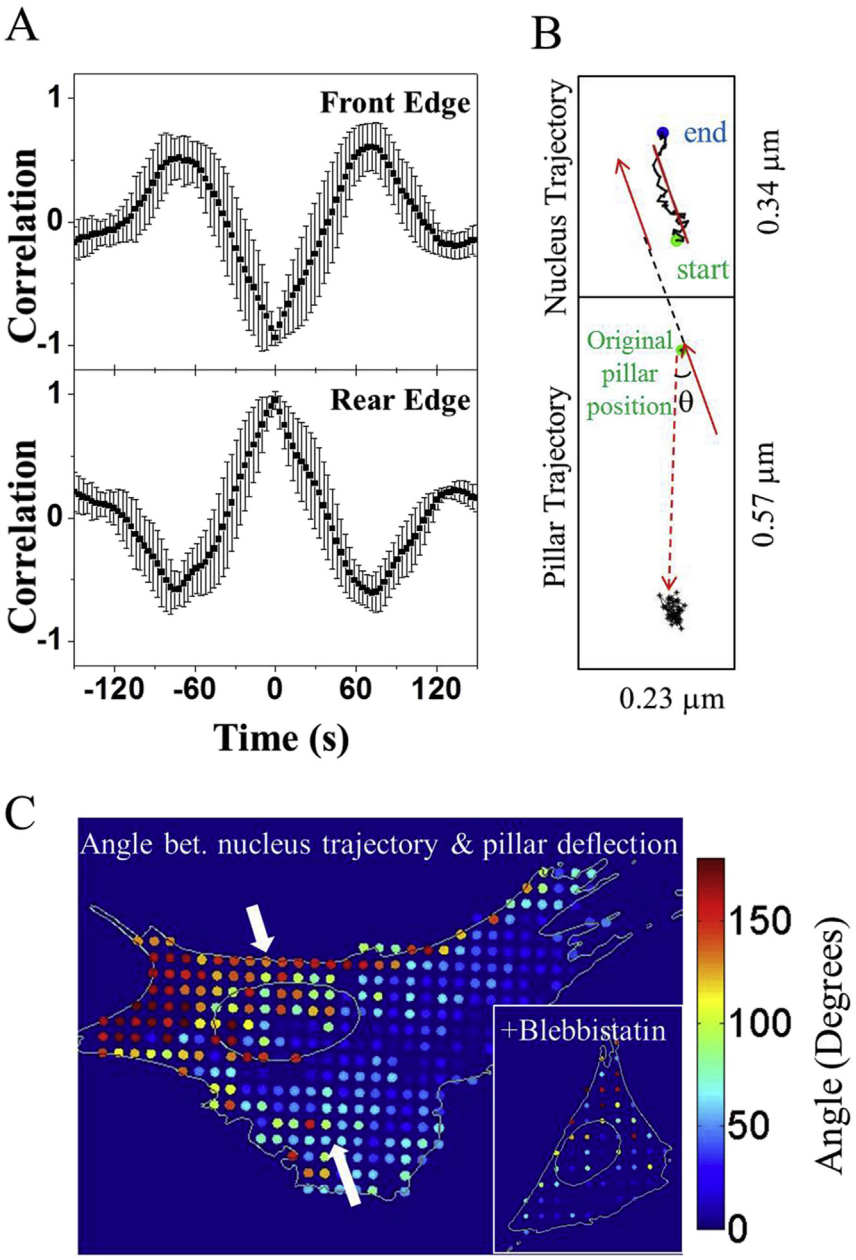

Fig. 4. Spatial cross-correlation analysis. (A) Cross correlation of front and rear edge pillar deflections with nucleus displacement (B) The best fit line of nucleus trajectory is the direction of nucleus movement. The direction of pillar deflection is defined from original pillar position to mean pillar position. (C) Color coded angle between nucleus trajectory and pillar deflection, depicting that fluctuations of pillars at leading edge of migrating cell are opposite to direction of nucleus displacement (negative correlation) while those of pillars at the lagging end are in the same direction (positive correlation). Inset shows loss of correlation upon blebbistatin treatment.

Author contributions

Q.L., E.M. and G.V.S. designed experiments. Q.L., E.M. and F.M.H. performed experiments and analysis. All authors wrote and reviewed the manuscript.

Conflict of interest

None.

Acknowledgments

We thank Mechanobiology Institute for financial support. We also thank CT.Lim and Benoit Ladoux's laboratories for sharing micropillar moulds and useful discussions.

Transparency document

Transparency document related to this article can be found online at http://dx.doi.org/10.1016/j.bbrc.2015.04.041.

Appendix A. Supplementary data

Supplementary data related to this article can be found at http://dx.doi.org/10.1016/j.bbrc.2015.04.041.

References

[1] V. Vogel, M. Sheetz, Local force and geometry sensing regulate cell functions, Nat. Rev. Mol. Cell. Biol. 7 (4) (2006) 265–275.
[2] A.J. Engler, S. Sen, H.L. Sweeney, D.E. Discher, Matrix elasticity directs stem cell lineage specification, Cell 126 (4) (2006) 677–689.

[3] K.A. Kilian, B. Bugarija, B.T. Lahn, M. Mrksich, Geometric cues for directing the differentiation of mesenchymal stem cells, Proc. Natl. Acad. Sci. U. S. A. 107 (11) (2010) 4872–4877.
[4] N. Jain, K.V. Iyer, A. Kumar, G.V. Shivashankar, Cell geometric constraints induce modular gene-expression patterns via redistribution of HDAC3 regulated by actomyosin contractility, Proc. Natl. Acad. Sci. U. S. A. 110 (28) (2013) 11349–11354.
[5] N. Desprat, W. Supatto, P.A. Pouille, E. Beaurepaire, E. Farge, Tissue deformation modulates twist expression to determine anterior midgut differentiation in Drosophila embryos, Dev. Cell. 15 (3) (2008) 470–477.
[6] B. Geiger, J.P. Spatz, A.D. Bershadsky, Environmental sensing through focal adhesions, Nat. Rev. Mol. Cell. Biol. 10 (1) (2009) 21–33.
[7] A.J. Maniotis, C.S. Chen, D.E. Ingber, Demonstration of mechanical connections between integrins, cytoskeletal filaments, and nucleoplasm that stabilize nuclear structure, Proc. Natl. Acad. Sci. U. S. A. 94 (3) (1997) 849–854.
[8] S. Na, O. Collin, F. Chowdhury, B. Tay, M. Ouyang, Y. Wang, N. Wang, Rapid signal transduction in living cells is a unique feature of mechanotransduction, Proc. Natl. Acad. Sci. U. S. A. 105 (18) (2008) 6626–6631.
[9] G.V. Shivashankar, Mechanosignaling to the cell nucleus and gene regulation, Annu Rev. Biophys. 40 (2011) 361–378.
[10] M.L. Lombardi, D.E. Jaalouk, C.M. Shanahan, B. Burke, K.J. Roux, J. Lammerding, The interaction between nesprins and sun proteins at the nuclear envelope is critical for force transmission between the nucleus and cytoskeleton, J. Biol. Chem. 286 (30) (2011) 26743–26753.
[11] K.V. Iyer, S. Pulford, A. Mogilner, G.V. Shivashankar, Mechanical activation of cells induces chromatin remodeling preceding MKL nuclear transport, Biophys. J. 103 (7) (2012) 1416–1428.
[12] E.A. Booth-Gauthier, T.A. Alcoser, G. Yang, K.N. Dahl, Force-induced changes in subnuclear movement and rheology, Biophys. J. 103 (12) (2012) 2423–2431.
[13] S.B. Khatau, C.M. Hale, P.J. Stewart-Hutchinson, M.S. Patel, C.L. Stewart, P.C. Searson, D. Hodzic, D. Wirtz, A perinuclear actin cap regulates nuclear shape, Proc. Natl. Acad. Sci. U. S. A. 106 (45) (2009) 19017–19022.
[14] G.W. Luxton, E.R. Gomes, E.S. Folker, E. Vintinner, G.G. Gundersen, Linear arrays of nuclear envelope proteins harness retrograde actin flow for nuclear movement, Science 329 (5994) (2010) 956–959.
[15] A.B. Chambliss, S.B. Khatau, N. Erdenberger, D.K. Robinson, D. Hodzic, G.D. Longmore, D. Wirtz, The LINC-anchored actin cap connects the extracellular milieu to the nucleus for ultrafast mechanotransduction, Sci. Rep. 3 (2013) 1087.
[16] B. Burke, C.L. Stewart, The nuclear lamins: flexibility in function, Nat. Rev. Mol. Cell. Biol. 14 (1) (2013) 13–24.
[17] Q. Li, A. Kumar, E. Makhija, G.V. Shivashankar, The regulation of dynamic mechanical coupling between actin cytoskeleton and nucleus by matrix geometry, Biomaterials 35 (3) (2014) 961–969.
[18] J.L. Tan, J. Tien, D.M. Pirone, D.S. Gray, K. Bhadriraju, C.S. Chen, Cells lying on a bed of microneedles: an approach to isolate mechanical force, Proc. Natl. Acad. Sci. U. S. A. 100 (4) (2003) 1484–1489.
[19] A. Jasaitis, M. Estevez, J. Heysch, B. Ladoux, S. Dufour, E-cadherin-dependent stimulation of traction force at focal adhesions via the Src and PI3K signaling pathways, Biophys. J. 103 (2) (2012) 175–184.
[20] M. Ghibaudo, A. Saez, L. Trichet, A. Xayaphoummine, J. Browaeys, P. Silberzan, et al., Traction forces and rigidity sensing regulate cell functions, Soft Matter 4 (2008) 1836–1843.
[21] C.G. Galbraith, M.P. Sheetz, A micromachined device provides a new bend on fibroblast traction forces, Proc. Natl. Acad. Sci. U. S. A. 94 (17) (1997) 9114–9118.
[22] N. Wang, J.D. Tytell, D.E. Ingber, Mechanotransduction at a distance: mechanically coupling the extracellular matrix with the nucleus, Nat. Rev. Mol. Cell. Biol. 10 (1) (2009) 75–82.
[23] J.S. Lee, C.M. Hale, P. Panorchan, S.B. Khatau, J.P. George, Y. Tseng, C.L. Stewart, D. Hodzic, D. Wirtz, Nuclear lamin A/C deficiency induces defects in cell mechanics, polarization, and migration, Biophys. J. 93 (7) (2007) 2542–2552.
[24] M.L. Gardel, B. Sabass, L. Ji, G. Danuser, U.S. Schwarz, C.M. Waterman, Traction stress in focal adhesions correlates biphasically with actin retrograde flow speed, J. Cell. Biol. 183 (6) (2008) 999–1005.
[25] M. Guo, A.J. Ehrlicher, M.H. Jensen, M. Renz, J.R. Moore, R.D. Goldman, J. Lippincott-Schwartz, F.C. Mackintosh, D.A. Weitz, Probing the stochastic, motor-driven properties of the cytoplasm using force spectrum microscopy, Cell 158 (4) (2014) 822–832.